

# Thermal design of spiral heat exchangers and heat pipes through global best algorithm

Oğuz Emrah Turgut<sup>1</sup> · Mustafa Turhan Çoban<sup>1</sup>

Received: 1 January 2016 / Accepted: 21 June 2016 / Published online: 7 July 2016  
© Springer-Verlag Berlin Heidelberg 2016

**Abstract** This study deals with global best algorithm based thermal design of spiral heat exchangers and heat pipes. Spiral heat exchangers are devices which are highly efficient in extremely dirty and fouling process duties. Spirals inherent in design maintain high heat transfer coefficients while avoiding hazardous effects of fouling and uneven fluid distribution in the channels. Heat pipes have wide usage in industry. Thanks to the two phase cycle which takes part in operation, they can transfer high amount of heat with a negligible temperature gradient. In this work, a new stochastic based optimization method global best algorithm is applied for multi objective optimization of spiral heat exchangers as well as single objective optimization for heat pipes. Global best algorithm is easy-to-implement, free of derivatives and it can be reliably applied to any optimization problem. Case studies taken from the literature approaches are solved by the proposed algorithm and results obtained from the literature approaches are compared with those acquired by GBA. Comparisons reveal that GBA attains better results than literature studies in terms of solution accuracy and efficiency.

## List of symbols

A	Heat transfer area (m <sup>2</sup> )
b	Channel spacing (m)
c	Specific heat (J/kg K)
C	Core diameter (m)
C <sub>E</sub>	Energy cost (€/kWh)
C <sub>i</sub>	Investment cost (€)

C <sub>od</sub>	Total discounted operating cost (€)
C <sub>o</sub>	Annual operating cost (€/year)
C <sub>tot</sub>	Total cost (€)
d	Wick wire diameter (m)
d <sub>i</sub>	Heat pipe internal diameter (m)
d <sub>o</sub>	Heat pipe external diameter (m)
d <sub>v</sub>	Diameter of vapor core (m)
D <sub>h</sub>	Average hydraulic diameter of channel (m)
D	Outside spiral diameter (m)
F	Frictional coefficient (N/Wm)
g	Gravitational acceleration, 9.81 (m/s <sup>2</sup> )
G	Mass flux (kg/m <sup>2</sup> s)
h	Heat transfer coefficient (W/m <sup>2</sup> K)
h <sub>fg</sub>	Latent heat of vaporization (J/kg)
H	Plate width (m)
HW	Annual operating time (h/year)
i	Annual discount rate
k, k <sub>l</sub>	Thermal conductivity of the working fluid (W/mK)
k <sub>eff</sub>	Effective thermal conductivity of the wick (W/mK)
k <sub>p</sub>	Thermal conductivity of the plate (W/mK)
k <sub>t</sub>	Thermal conductivity of the heat pipe wall (W/mK)
k <sub>w</sub>	Thermal conductivity of the heat pipe wick material (W/mK)
L	Plate length (m)
L <sub>a</sub>	Adiabatic section length (m)
L <sub>c</sub>	Condenser section length (m)
L <sub>e</sub>	Evaporator section length (m)
L <sub>eff</sub>	Heat pipe effective length (m)
L <sub>total</sub>	Total heat pipe length (m)
LMTD	Logarithmic mean temperature difference (K)
M <sub>v</sub>	Mach number at vapor core
m <sub>cont</sub>	Mass of the container (kg)

✉ Oğuz Emrah Turgut  
oeturgut@hotmail.com

<sup>1</sup> Mechanical Engineering Department, Ege University,  
35040 Bornova, İzmir, Turkey

$m_{\text{vapor}}$	Mass of the fluid vapor flowing inside the heat pipe (kg)
$m_{\text{wd}}$	Mass of the dry wick (kg)
$m_{\text{wl}}$	Mass of the liquid wick (kg)
$\dot{m}$	Mass flow rate (kg/s)
$N$	Wick's mesh number (1/m)
$Nu$	Nusselt number
$n_y$	Equipment life (year)
$P$	Pumping power (W)
$P_{\text{amb}}$	Ambient pressure outside the heat pipe (Pa)
$P_c$	Capillary pressure (Pa)
$P_g$	Hydrostatic pressure (Pa)
$Pr$	Prandtl number
$\Delta P$	Pressure drop (kPa)
$Q$	Heat load, heat transfer rate (W)
$Q_b$	Boiling limit (W)
$Q_c$	Capillary limit (W)
$Q_e$	Entrainment limit (W)
$Q_v$	Viscous limit (W)
$r_c$	Capillary radius (m)
$r_n$	Nucleation radius (m)
$r_{h,s}$	Hydraulic radius for wick surface pores (m)
$r_v$	Vapor core radius (m)
$R$	Spiral radius (m)
$R$	Thermal resistance (K/W)
$R$	Ideal gas constant (J/kgK)
$R_{\text{ct}}$	Thermal resistance of the heat pipe wall at the condenser section (K/W)
$R_{\text{cw}}$	Thermal resistance of the heat pipe wick at the condenser section (K/W)
$R_{\text{et}}$	Thermal resistance of the heat pipe wall at the evaporator section (K/W)
$R_{\text{ew}}$	Thermal resistance of the heat pipe wick at the evaporator section (K/W)
$R_f$	Fouling factor (W/m <sup>2</sup> K)
$Re$	Reynolds number
$t$	Plate thickness (m)
$t_t$	Heat pipe tube thickness (m)
$t_w$	Heat pipe wick thickness (m)
$T$	Temperature (K)
$T_{\text{si}}$	Temperature on the outside wall of the condenser section (K)
$T_{\text{so}}$	Temperature on the outside wall of the evaporator section (K)
$T_v$	Saturated vapor temperature (K)
$u_{\text{ts}}$	Ultimate tensile strength of the wall material of the heat pipe (Pa)
$U$	Overall heat transfer coefficient (W/m <sup>2</sup> K)
$V$	Mean velocity of the working fluid (m/s)

### Greek symbols

$\alpha$	Inclination angle
$\gamma_v$	Specific heat ratio

$\varepsilon$	Porosity
$\eta$	Pumping efficiency
$\mu$	Viscosity (kg/ms)
$\rho$	Density (kg/m <sup>3</sup> )
$\sigma$	Surface tension (N/m)

### Subscripts

$c$	Cold stream
$\text{cont}$	Container
$h$	Hot stream
$i$	Inlet
$l$	Liquid phase
$\text{max}$	Maximum
$\text{min}$	Minimum
$o$	Outlet
$v$	Vapor phase
$w$	Wick structure

## 1 Introduction

Researchers are greatly encouraged by the new emerging technologies to create new arrangements and artifacts in engineering design. Worldwide competition in terms of efficient design of engineering systems has been drawn attention by the leading industries to accomplish their goals which pave the way for better improvements. However, increasing the quality of the products which perform the desired task may not satisfy the user's recognized needs. It is beneficial to optimize the total process by stating a relevant objective function if it is to maximize the system performance or to minimize the losses occurred in the system. Therefore, today's trending "hot spot" research topic, optimum design has become more and more indispensable not only for the designers who are involved in the pursuit of developing preferable system configurations but also for the customers who are seeking alternative options for their needs.

Amongst the mechanical systems those ruling everyday life, thermal systems have been abundantly used and utilized in many engineering fields such as power generation, air conditioning, material science, and automobile engineering etc. Therefore, researchers should focus on the optimum design of the thermal systems as they are obliged to apply optimization procedures to improve the quality of the products which are involved with industries ranging from transmission to robotics. After constructing a reliable mathematical model based on the physical attributes of the thermal system, a designer can easily upgrade the system performance by virtue of the selected optimization method. Application of optimization techniques allows designers to model a system with a minimum cost whilst meeting required constraints. Designer have plenty of options

in selecting a proper optimization algorithm. Traditional optimization methods (Newton based methods, dynamic programming, etc.) have the ability of coping with the nonlinearities of the objective function however, they are prone to get stuck in the local optimum points in the search space. Moreover, they have experienced difficulties in handling hard-to-solve equality and inequality constraints imposed on the optimization problem. As a promising alternative to conventional methods, metaheuristic algorithms such as Genetic Algorithm [1–7], Differential Evolution [8–11], Artificial Bee Colony algorithm [12–14], and Particle Swarm Optimization [15–18] have been widely used to overcome the obstacles in modelling the efficient design of thermal and energy systems. Metaheuristic methods are based on the stochastic optimization so that optimal solution found is in the effect of random variables used in the search process. They often find feasible solutions with less computational burden compared to the iterative methods. They are usually non-deterministic, not problem specific, and they tend to find near-optimal solutions due to their stochastic nature [19].

As an important part of thermal systems, heat exchangers are widely used in various industries. Heat exchanger is used for the effective heat transfer between two (or more) working fluids from one to another. Among the various type of heat exchangers available in the market, spiral heat exchangers have gained an important seat in its industry. Spiral heat exchangers were firstly introduced in 19th century [20]. Their usage is ideal for the cooling slurries and viscous fluids. They can achieve high convective heat transfer rates due to spiral pattern which sustain turbulent flow in the heat exchanger. They have common applications in the area of paper, petrochemical, food and sugar industries in evaporation and condensation [21]. These favorable characteristics make them highly relevant to utilization in thermal systems. A typical representation of a spiral heat exchanger is given in Fig. 1. There are plenty of studies concerning the utilization of spiral heat exchangers in various areas of the energy systems. Wilhelmson [22] identified the working principles and the industrial applications of the spiral heat exchangers. Picun-Nunez [23, 24] described the basics of the sizing of the spiral type heat exchangers. Naphon and Wongwises [25] investigated the average in-tube flow heat transfer coefficients in a spiral coil. Effects of the inlet conditions of the two working fluids were identified. Experimental results were compared with those obtained from the correlations available in the literature. Bebs and Roetzel [26] developed analytical model for the accurate calculation of the temperature changes in counter-current flow spiral heat exchangers. Li et al. [27] proposed an innovative methodology for analyzing the heat transfer performance of a spiral heat exchanger. Burmeister [28] put forward a solution strategy to identify the dependence

of the heat transfer effectiveness on the number of transfer units for a spiral heat exchanger. Lu et al. [29] analyzed the shell-side-flow and heat transfer performance of multilayer spiral wound heat exchanger under turbulence flow conditions by carrying out experimental studies and numerical procedures.

Heat pipes are the essential elements of the thermal energy systems. Heat pipes were come into use at the later stages of 1940s, however their general utilization in energy systems started in mid-1960s [30]. Heat pipes are devices which transports high amount of energy from a heat source to a heat sink with a negligible temperature gradient by means of the latent heat of vaporization of the working fluid. They work under high thermal conductivities, have the ability to transport massive heat loads over long distances, and are vibration-free in operation [31]. Basically, heat pipe is a tube-type component having a working fluid on its core with a wick structure filled with the working fluid which is designed to sustain capillary action for the saturated liquid. A typical heat pipe consists of three distinct operation units: an evaporator unit, an adiabatic (heat transport) unit, and a condenser unit as depicted in Fig. 2.

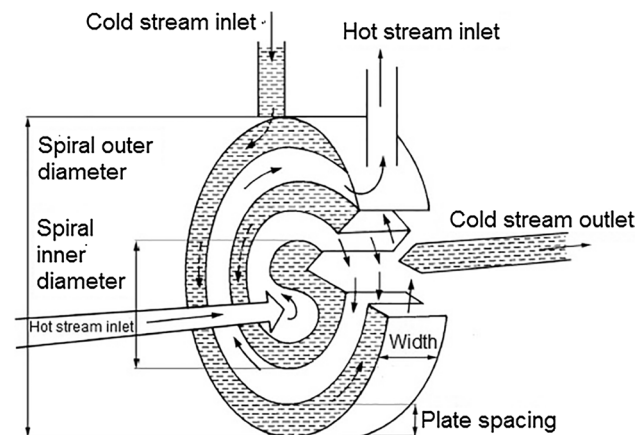


**Fig. 1** Flow pattern and geometrical features of a spiral heat exchanger [44]

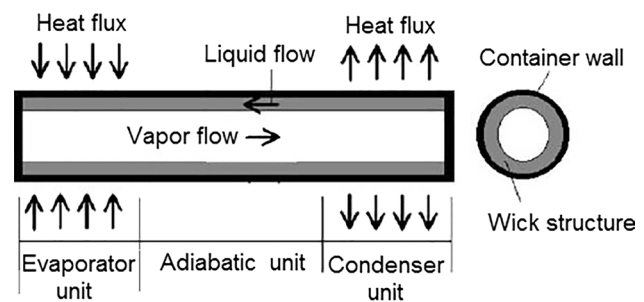


**Fig. 2** Schematic representation of a conventional heat pipe [47]

Supplied heat at the evaporator section, which vaporizes the working fluid, is transported throughout the adiabatic section. As the working fluid in the form of vapor reaches the condenser section, releases its present latent heat and becomes liquified. The liquid enters the wick structure, leaves the condenser and moves through the evaporator by means of the capillary forces exerted on it by the pressure difference in the system.

There are numerous research studies in the literature concerning the design procedure of the heat pipes. Said and Akash [32] experimentally studied two different heat pipes using water as a working fluid. One heat pipe having a wick and one having no wick. They positioned the heat pipes at different angles of 30°, 60° and 90° with the horizontal. Results showed that the heat pipe with having a wick structure shows better performance than having no wick in terms of overall heat transfer coefficient. Kim et al. [33] developed a heat and mass transfer model for a miniature heat pipe with a grooved wick structure and solved analytically in order for obtaining the maximum heat transport rate and overall thermal resistance under steady-state. Shi et al. [34], made numerical analysis based performance evaluation of miniature heat pipes in low temperature cofire ceramic (LTCC) substrates. They fabricated simple prototype of a LTCC and discussed the effect of the grooved depth, width and vapor space on the total heat transfer capacity and efficiency of the miniature heat pipe. Vlassov et al. [35] used Generalized Extremal Optimization algorithm to design the optimal mass characteristics of a heat pipe radiator assembly, which was aimed to be utilized in space radiator assembly. Maheshkumar and Muraleedharan [36] presented a mathematical model to minimize the total entropy generation in a flat heat pipe. Agha [37] used Taguchi method to analyze the effect of the heat pipe design parameters including wick structure, heat pipe diameter, and working fluid on the total system performance. Lips and Lefevre [38] developed a generalized analytical model based on Fouries series expansion for solution of 3D temperature field and 2D pressure and velocity fields within a conventional heat pipe. Cui et al. [39] experimentally studied a closed-loop pulsating heat pipe four types of working fluids including deionized water, methanol, ethanol and acetone. Nithyanandam and Pitchumani [40] embedded heat pipes into latent thermal energy storage system (LTES) in order to reduce the thermal resistance of LTES by augmenting the energy transfer from the working fluid to the phase change material.

As seen from the literature survey, there are various studies which were devoted to optimize the performance of the spiral heat exchangers and heat pipes. Some researchers have used sophisticated optimization techniques in successful and efficient modelling of heat pipes [35, 41–43] and spiral heat exchangers [44]. However, results of

the concerning studies showed that there is still room to improve the best solutions in terms of solution accuracy. In this study, a new optimization method, global best algorithm (GBA) is proposed to achieve the optimal design of these thermal system components. GBA uses some of the manipulation schemes of the Differential Evolution [45] algorithm and tries to obtain the optimum solution of the objective function by avoiding get trapped of in local optimum points. GBA probes the search space by guidance of the global best solution obtained so far on the course of iterations and requires fewer algorithm parameters which are very crucial in deciding the robustness of any optimization algorithm. In the present work, optimum geometric parameters of spiral heat exchangers will be obtained through multi objective GBA (MO-GBA) as well as satisfying conflicting objectives simultaneously. Case study obtained from Moretta [46] will be solved by the proposed GBA in order to obtain optimum design parameters of the spiral heat exchanger within allowable pressure drops and design constraints. Moreover, as an application of real world optimization problem, a heat pipe used for space applications will be optimized by GBA with respect to its total mass. Optimization problem possess serious difficulties to GBA with a harshly nonlinear objective function and eighteen binding constraints including operational, dimensional and structural ones. Working fluid properties of the heat pipe are assumed temperature dependent and steady state conditions are considered for the calculations.

## 2 Mathematical modelling

### 2.1 Formulation of the heat pipe design problem

Heat pipe modeled in this section is used in space applications. In this kind of applications, total mass of the space platform should be as low as possible [47]. This case study, previously solved by Rao and More [31] and Souza et al. [47], aims to optimize the geometric parameters of the constant conductance type heat pipe to be used in the thermal control subsystem of a satellite. Methanol is used as a working fluid. Material of the container is selected as a stainless steel (SS304) since it can work with all type of working fluids [31]. Mesh type wick structure is utilized, which is also made of stainless steel.

Based on the imposed working conditions, objective of the design problem is to minimize total mass of the heat pipe subjected to various kinds of constraints. In order to accomplish a heat pipe design with obeying the imposed constraints, structural decision variables including the wick diameter ( $d$ ), the wick's mesh number ( $N$ ), the wick thickness ( $t_w$ ), vapor core diameter ( $d_v$ ), the thickness of the container's wall ( $t_c$ ), the length of the evaporator section ( $L_e$ ),

and the length of the condenser section ( $L_c$ ) are selected to be optimized. Therefore, formulation of the optimization problem can be expressed as:

Minimize

$$m_{total} = m_{cont} + m_{wd} + m_{wl} + m_{vapor} \quad (1)$$

where

$$m_{cont} = \pi d_t (d_i + t_t) \rho_t L_{total} \quad (2)$$

$$m_{wd} = \pi t_w (d_v + t_w) (1 - \varepsilon) \rho_w L_{total} \quad (3)$$

$$m_{wl} = \pi t_w (d_v + t_w) \varepsilon \rho_l L_{total} \quad (4)$$

$$m_{vapor} = \frac{\pi d_v^2 \rho_v L_{total}}{4} \quad (5)$$

where  $m_{cont}$  is the mass of the container,  $m_{wd}$  is the mass of the dry wick,  $m_{wl}$  is the mass of the saturated liquid in the wick, and  $m_{vapor}$  is the mass of the saturated vapor in the heat pipe. As it was mentioned before, optimization problem is subjected to eighteen constraints which are formulated below [31, 47].

$$G_1 : Q \leq Q_c \quad (6)$$

where

$$Q_c = \frac{P_c + P_g}{(F_l + F_v) L_{eff}} \quad (7)$$

$$P_c = \frac{2\sigma}{r_c} \quad (8)$$

$$r_c = \frac{1}{2N} \quad (9)$$

$$P_g = \rho_l g [L_{total} \sin(\alpha) - d_v \cos(\alpha)] \quad (10)$$

$$F_l = \frac{\mu_l}{K \left( \pi \frac{d_i^2 - d_v^2}{4} \right) \rho_l} \quad (11)$$

$$K = \frac{d^2 \varepsilon^3}{122(1 - \varepsilon)^2} \quad (12)$$

$$\varepsilon = 1 - \frac{1.05\pi Nd}{4} \quad (13)$$

$$F_v = \frac{128\mu_v}{\pi d_v^4 \rho_v h_{fg}} \quad (14)$$

$$L_{eff} = \frac{L_e + L_c}{2} + L_a \quad (15)$$

$$d_i = d_v + 2t_w \quad (16)$$

$$G_2 : T_{somin} \leq T_{so} \leq T_{somax} \quad (17)$$

where  $T_{so}$  is temperature of the heat source at the external wall of the evaporator section. For electronic components used in space applications, operating limits in terms of working temperature are generally ranged between  $T_{somin} = -10.0$  °C and  $T_{somax} = 45.0$  °C which are selected as upper and lower bounds for the present problem. The temperature  $T_{so}$  can be found by the thermal balance between the condenser section and the evaporator section of the heat pipe with the expression given below:

$$T_{so} = RQ + T_{si} \quad (18)$$

where

$$R = R_{et} + R_{ct} + R_{ew} + R_{cw} \quad (19)$$

$$R_{et} = \frac{\ln\left(\frac{d_o}{d_i}\right)}{2\pi L_e k_t} \quad (20)$$

$$R_{ct} = \frac{\ln\left(\frac{d_o}{d_i}\right)}{2\pi L_c k_t} \quad (21)$$

$$R_{ew} = \frac{\ln\left(\frac{d_i}{d_v}\right)}{2\pi L_e k_{eq}} \quad (22)$$

$$R_{cw} = \frac{\ln\left(\frac{d_i}{d_v}\right)}{2\pi L_c k_{eq}} \quad (23)$$

$$k_{eq} = \frac{k_l [(k_l + k_w) - (1 - \varepsilon)(k_l - k_w)]}{[(k_l + k_w) + (1 - \varepsilon)(k_l - k_w)]} \quad (24)$$

$$G_3 : Q \leq Q_b \quad (25)$$

where

$$Q_b = \frac{2\pi L_e k_{eq} T_v}{\rho_v h_{fg} \ln\left(\frac{d_i}{d_v}\right)} \left( \frac{2\sigma}{r_n} - P_c \right) \quad (26)$$

$$G_4 : Q \leq Q_e \quad (27)$$

where

$$Q_e = \frac{\pi d_v^2 h_{fg}}{4} \sqrt{\left( \frac{\sigma \rho_v}{\left( \frac{1}{N} - d \right)} \right)} \quad (28)$$

$$G_5 : Q \leq Q_v \quad (29)$$

where

$$Q_v = \frac{\pi d_v^4 \rho_v h_{fg} P_v}{256 \mu_v L_{eff}} \quad (30)$$

$$G_6 : M_v \leq 0.2 \quad (31)$$

where

$$M_v = \frac{8Q}{\pi d_v^3 h_{fg} \sqrt{\gamma_v R_v T_v}} \quad (32)$$

$$G_7 : \text{Re}_v \leq 2300 \quad (33)$$

where

$$\text{Re}_v = \frac{4Q}{\pi d_v \mu_v h_{fg}} \quad (34)$$

$$G_8 : 0.0001 \leq \varepsilon \leq 0.9999 \quad (35)$$

$$G_9 : 2d \leq t_w \quad (36)$$

$$G_{10} : 314 \leq N \leq 15000 \quad (37)$$

$$G_{11} : 0.025 \cdot 10^{-3} \leq d \leq 1.0 \cdot 10^{-3} \quad (38)$$

$$G_{12} : 5.0 \cdot 10^{-3} \leq d_v \leq 80.0 \cdot 10^{-3} \quad (39)$$

$$G_{13} : 0.05 \cdot 10^{-3} \leq t_w \leq 10.0 \cdot 10^{-3} \quad (40)$$

$$G_{14} : 50.0 \cdot 10^{-3} \leq L_e \leq 400.0 \cdot 10^{-3} \quad (41)$$

$$G_{15} : 50.0 \cdot 10^{-3} \leq L_c \leq 400.0 \cdot 10^{-3} \quad (42)$$

$$G_{16} : 0.3 \cdot 10^{-3} \leq t_t \leq 3.0 \cdot 10^{-3} \quad (43)$$

$$G_{17} : \frac{\Delta P (d_o^2 + d_i^2)}{d_o^2 - d_i^2} \leq \frac{u_{ts}}{4} \quad (44)$$

where  $\Delta P = P_v - P_{amb}$ ,  $P_{amb} = 0$  as the heat pipe operates in vacuum.

$$G_{18} : \frac{\Delta P (d_o^3 + 2d_i^3)}{2(d_o^3 - d_i^3)} \leq \frac{u_{ts}}{4} \quad (45)$$

## 2.2 Formulation of the spiral heat exchanger design problem

Based on the case study given in Moretta [46], spiral heat exchanger design problem will be implemented in this section. In order to maintain simplicity in calculations, heat losses to the surroundings are assumed to be negligible. Obeying the rules of the first law of thermodynamics, heat

balance between hot and cold side can be constructed by the following expression.

$$Q = m_h c_h (T_{hi} - T_{ho}) = m_c c_c (T_{co} - T_{ci}) \quad (46)$$

Using LMTD and overall heat transfer coefficient,  $U$ , the heat transfer rate for the spiral heat exchanger can also be expressed as:

$$Q = U \cdot A \cdot LMTD \quad (47)$$

The overall heat transfer coefficient,  $U$ , can be calculated as:

$$U = \frac{1}{\frac{1}{h_h} + \frac{t}{k_p} + \frac{1}{h_c} + R_f} \quad (48)$$

Logarithmic mean temperature difference is calculated by the following formula:

$$LMTD = \frac{(T_{hi} - T_{co}) - (T_{ho} - T_{ci})}{\ln \left( \frac{T_{hi} - T_{co}}{T_{ho} - T_{ci}} \right)} \quad (49)$$

Total heat transfer area is determined by the following equation:

$$A = 2LH \quad (50)$$

Film heat transfer coefficient in a spiral plate heat exchanger is calculated from the correlation of Morimoto and Hotta [48]

$$Nu = 0.0239 \left( 1 + 5.54 \frac{D_h}{R_m} \right) \text{Re}^{0.806} \text{Pr}^{0.286} \quad (51)$$

where  $D_h$  is the average hydraulic diameter expressed as:

$$D_h = \frac{2HS}{H+S} \quad (52)$$

The spiral diameter ( $R_m$ ) is determined by:

$$R_m = \frac{R_{\min} + R_{\max}}{2} \quad (53)$$

Reynolds and Prandtl numbers are calculated by the following expressions:

$$\text{Re} = \frac{GD_h}{\mu} \quad (54)$$

$$\text{Pr} = \frac{C_p \mu}{k} \quad (55)$$

where  $G$  is the mass flux calculated by the following:

$$G = \frac{\dot{m}}{A} = \frac{\dot{m}}{HS} \quad (56)$$

Pressure drop in spiral heat exchanger is formulated by the expression given below [49]:

$$\Delta P = \frac{1.45(LV^2\rho)}{1705 \times 10^3} \quad (57)$$

where  $V$  is the mean velocity expressed as:

$$V = \frac{G}{\rho} \quad (58)$$

The outside spiral diameter is calculated from the equation defined as [50]:

$$D_s = \left[ 1.28L(b_h + b_c + 2t) + C^2 \right]^{0.5} \quad (59)$$

Total cost of heat exchanger is determined by:

$$C_{tot} = C_i + C_{od} \quad (60)$$

where  $C_i$  accounts for the manufacturing costs of heat exchanger, which is calculated through Hall equation [51], is calculated as follows:

$$C_i = 5873A^{0.59} \quad (61)$$

Second term in Eq. (60),  $C_{od}$ , stands for the operational costs made by pressure losses caused through friction and is calculated by the following expression

$$C_{od} = \sum_{i=1}^{ny} \frac{C_o}{(1+i)^k} \quad (62)$$

$$C_o = P \cdot C_E \cdot HW \quad (63)$$

$$P = \frac{1}{\eta} \left( \frac{\dot{m}_h}{\rho_h} \Delta P_h + \frac{\dot{m}_c}{\rho_c} \Delta P_c \right) \quad (64)$$

In Eqs. (60)–(64), overall pumping efficiency is considered as 0.75, and annual amount of work hours is  $HW = 8000$  h/year. Discounted operating costs are computed with the energy cost ( $C_E$ ) of 0.12 €/kW h, equipment life is taken as  $ny = 15$  years, and annual discount rate is considered as  $i = 10\%$ .

This design problem also inherits several equality and inequality constraints including pressure drops in hot and cold sides, heat duty imposed on the system, and equality expression related to outer diameter. These conflicting nonlinear constraints are put into practice to achieve the desired working conditions and are formulated by the following expressions.

1. Hot side pressure drop constraint:

$$\Delta P_h \leq \frac{1.45LV^2\rho_h}{1705} \quad (65)$$

2. Cold side pressure drop constraint:

$$\Delta P_c \leq \frac{1.45LV^2\rho_c}{1705} \quad (66)$$

3. Outer diameter constraint:

$$D_s^2 - \left[ C^2 + (15.36L(b_h + b_b + t)) \right] = 0 \quad (67)$$

4. Heat transfer constraint:

$$Q - (U \cdot A \cdot LMTD) = 0 \quad (68)$$

### 3 Global best algorithm

This study proposes a new metaheuristic algorithm based on the global best solution obtained on the course of iterations. The proposed algorithm, which is developed by the authors of this study, takes the full advantage of this solution vector, utilizes it during the vector manipulation process and probes around this vector in order to acquire better results. Algorithm consists of two distinct parts. First part of the algorithm uses random numbers generated by Logistic map [52], which was proposed by the renowned biologist Robert May in his paper and clearly explains how simple chaotic behavior arise from non-repetitive dynamical equations, in order to produce more effective results in terms of scattered population individuals over the search space and increase the exploration capacity of the algorithm. Chaotic sequences produced by Logistic map can be simply formulized as

$$y(t+1) = 4y(t)(1-y(t)), \quad y(t) \in (0, 1) \quad (69)$$

where  $y(0) \notin \{0, 0.25, 0.5, 0.75, 1.0\}$ . By this map, very long and ergodic random number sequences can be generated. Algorithm starts with initializing  $D$  dimensional  $N$  elements by the procedure given below

```
for i = 1 to N
  for j = 1 to D
     $X_{i,j} = low_j + (up_j - low_j) \times \phi_{i,j}$ 
  end
end
```

where  $X$  is the current  $N$ -sized  $D$  dimensional matrix;  $low$  and  $up$  respectively stand for the upper and lower bounds of the search space;  $\phi$  is the random number produced by Logistic map between 0.0 and 1.0. Algorithm follows with determining the global best solution for current population ( $G_{best}$ ). In the first part of the algorithm, population individuals are manipulated based on the current  $G_{best}$  solution by the given manipulation schemes below

$$V_{i,j} = G_{best,j} + (2.0 \times (\phi - 0.5)) \times (G_{best,j} - X_{i,j}) \quad (71)$$

$$V_{i,j} = G_{best,j} + (2.0 \times (\phi - 0.5)) \times (X_{new,i,j} - X_{i,j}) \quad (72)$$

where  $X_{new,i,j}$  is comprised of individuals formed by *randperm()* function which shuffles the row elements of the population members of  $X_{i,j}$  randomly. Individuals that go beyond previously prescribed search boundaries are updated by the Eq. (73) given as

$$\begin{aligned} & \text{if} \left( (X_{i,j} < low_j) \parallel (X_{i,j} > up_j) \right) \\ & \quad X_{i,j} = low_j + ((up_j - low_j) \times \phi) \end{aligned} \quad (73)$$

end

Second part of the algorithm uses general manipulation schemes of the DE algorithm [45] and focuses on the exploitation of the promising areas during the iterations. In this phase, crossover operation, which is also utilized in DE algorithm responsible for producing trial solution vector, is incorporated into DE mutation operators in order to increase the solution diversity with the scheme given below

$$u_{i,j} = \begin{cases} v_{i,j} & \text{if} ((rand(0, 1) < CR) \parallel (j = randint(1, D))) \\ x_{i,j} & \text{else} \end{cases} \quad (74)$$

$j = 1, 2, 3, \dots, D$

where  $x$  is the parent vector;  $v$  is the mutated vector, and  $u$  is the trial vector. Crossover rate (CR) is a user defined parameter between 0.0 and 1.0 and copies  $j$ th parameter of the mutated vector to trial vector if required conditions are met. The function *rand(0,1)* generates Gaussian random number within (0,1) and *randint(1, D)* function provides random integers between 1 and D. In this study, scale factor (F), a control parameter for scaling the difference vector, is set to  $F = 0.02 * rand(0,1)$  after several numerical investigations. Crossover rate (CR) is adjusted by the self-adaptation scheme proposed in Brest et al. [53]. This scheme proposes new algorithm parameters such as  $\tau_1$  and  $\tau_2$ . According to this scheme, if generated crossover rate (CR) value is smaller than that of  $\tau_2$  then CR is reset between 0.0 and 1.0 or else it remains same. Intensification on the conquered domains of the search space is performed by the most widely used mutation schemes of the DE algorithm:

$$DE/best/1 \quad X_{new,i,j} = G_{best,j} + F \times (X_{r_1,j} - X_{r_2,j}) \quad (75)$$

$$\begin{aligned} DE/best/2 \quad X_{new,i,j} = & G_{best,i,j} + F \times (X_{r_1} - X_{r_2}) \\ & + F \times (X_{r_3} - X_{r_4}) \end{aligned} \quad (76)$$

where  $r_1, r_2, r_3, r_4, r_5 \in [1, N]$  and  $i$  is the current index where  $r_1 \neq r_2 \neq r_3 \neq r_4 \neq r_5 \neq i$ .  $X_{best}$  is the global

best solution obtained so far. In recent years, new innovative perturbation techniques have emerged for DE so as to improve solution accuracy and convergence capability of the algorithm. Ensemble learning [54] is a favorable and prominent example for these techniques. In the context of ensemble learning, different solution strategies of DE variants are combined to form a single and firm perturbation scheme which aims to bypass the local optimum points faced on the course of iterations. However, selection of adequate solution strategy for each population individual can be time consuming process which may require trial and error process that incurs heavily computational burden. Therefore, this study proposes the below procedure for manipulating population individuals.

```

for i = 1 to N
  if i % 2 == 0
    Apply DE/best/1 to  $X_i$ 
  else
    Apply DE/best/2 to  $X_i$ 
  end
end
    
```

(77)

where  $N$  is the size of the population;  $X_i$  is the  $i$ th member of the population and *rand(0,1)* is the Gaussian random number between 0.0 and 1.0. By this scheme, algorithm aims to explore the unvisited part of the search space and improve the solution accuracy with taking full advantage of the ensemble learning method. Pseudo-code of the proposed algorithm is explicitly described in Table 1.

### 4 Simulation results

This study aspires to demonstrate the effectivity and efficiency of the proposed global best algorithm in design of thermal energy systems. For this aim, successful design of spiral heat exchangers and heat pipes are selected as a suitable objective for modelling these kind of applications. Due to the stochastic nature of the GBA, 50 algorithm runs along with 20,000 function evaluations are taken into account and best result among the obtained solutions is retained for each case. For spiral heat exchanger design, a case study previously solved by Bidabadi et al. [44] and Moretta [46] is evaluated by GBA. Best results are compared with those obtained from Artificial Cooperative Search (ACS) algorithm [55], Intelligent Tuned Harmony Search (ITHS) algorithm [56], Quantum behaved Particle Swarm Optimization (QPSO) [57, 58] in order to assess the performance of the proposed optimization method. For heat pipe design, case study formerly practised by Rao and More [31] and Souza et al. [47] will be solved by GBA.

**Table 1** Global best algorithm pseudo-code

---

```

Initialize algorithm parameters
 $f(x)$  = objective function ( $D$  - dimensional)
 $N$  = population size
Upper and lower bounds of the search space
Maximum number of iterations (maxiter)
Determine CR, F,  $\tau_1$  and  $\tau_2$ 
Initialize the population randomly by Eq. (70) ( $X_{i,j}$ )
Generate chaotic sequences produced by Logistic map ( $\phi_{i,j}$ )
Determine the best solution vector ( $G_{best}$ ) among the population
Set iteration counter (iter) = 1
While (iter < maxiter)
  for  $i = 1$  to  $N$ 
    for  $j = 1$  to  $D$ 
       $X_{trial,i,j} = G_{best,j} + (2.0 \times (\phi_{i,j} - 0.5)) \times (G_{best,j} - X_{i,j})$ 
    end
    end
    Employ boundary check with Eq. (73) and update the  $G_{best}$  vector
    Compare the objective function values of  $X$  and  $X_{trial}$  individuals
    If the fitness value of  $X_{trial}$  individuals are better than that of  $X$  then replace them
     $X_{new} = \text{randperm}(X)$ 
    Generate chaotic sequences produced by Logistic map ( $\phi_{i,j}$ )
    for  $i = 1$  to  $N$ 
      for  $j = 1$  to  $D$ 
         $X_{trial,i,j} = G_{best,j} + (2.0 \times (\phi_{i,j} - 0.5)) \times (X_{new} - X_{i,j})$ 
      end
    end
    Employ boundary check with Eq. (73) and update the  $G_{best}$  vector
    Compare the objective function values of  $X$  and  $X_{trial}$  individuals
    If the fitness value of  $X_{trial}$  individuals are better than that of  $X$  then replace them
    for  $i = 1$  to  $N$ 
      Determine Scaling Factor (F) and Crossover Rate (CR)
      Select population individuals such that  $i \neq r_1 \neq r_2 \neq r_3 \neq r_4$ 
      if ( $i \% 2 = 0$ )
         $j_{rand} = \text{randint}(1, D)$ 
        for  $j = 1$  to  $D$ 
          if ( $\text{rand}(0,1) < CR$ ) || ( $j = j_{rand}$ )
             $X_{trial,i,j} = G_{best,j} + F \times (X_{r1,j} - X_{r2,j})$ 
          end
        end
      else
         $j_{rand} = \text{randint}(1, D)$ 
        for  $j = 1$  to  $D$ 
          if ( $\text{rand}(0,1) < CR$ ) || ( $j = j_{rand}$ )
             $X_{trial,i,j} = G_{best,j} + F \times (X_{r1,j} - X_{r2,j}) + F \times (X_{r3,j} - X_{r4,j})$ 
          end
        end
      end
    end
    Employ boundary check with Eq. (73) and update the  $G_{best}$  vector
    Compare the objective function values of  $X$  and  $X_{trial}$  individuals
    If the fitness value of  $X_{trial}$  individuals are better than that of  $X$  then replace them
    Update chaotic sequences generated by Logistic map ( $\phi_{i,j}$ )
    Determine  $G_{best}$  solution
    iter++
  end
  Output  $G_{best}$  vector

```

---

#### 4.1 Multi objective optimization of spiral heat exchangers

Optimization of the spiral heat exchanger is a typical example of multi objective optimization problem. Multi objective optimization can be explained as a decision-making process which involves more than one optimization problem to be solved concurrently with a given problem-related

constraints. Based on the optimization method proposed in this study, Pareto frontier with ideal and nadir points in the search space is constructed. In Pareto frontier, each obtained solution is a trade-off among the set of consolidated solutions of various conflicting objectives. In the context of Pareto front, no solution is better than the other and there will not be any improvement in objectives if any of the solution moves to another point on the frontier.

**Table 2** Average physical properties of the working fluids [46]

	Hot stream	Cold stream
Mass flow rate (kg/s)	127.67	18.91
Inlet temperature (K)	298.60	283.15
Outlet temperature (K)	298.15	285.88
Heat capacity (J/kg K)	3768.12	4186.80
Thermal conductivity (W/m K)	0.6231	0.5815
Density (kg/m <sup>3</sup> )	1349.39	999.55
Plate thickness (m)	0.0032	0.0032
Internal diameter (m)	0.3048	0.3048
Plate spacing (m)	0.0318	0.0063

Consequently, in feasible solution region, there is no solution having better results compared to solutions on the Pareto frontier.

Considering the spiral heat exchanger design, two conflicting objective namely maximizing heat transfer coefficient and minimizing total cost of heat exchanger are considered simultaneously for multi-objective optimization. Problem at hand is hard-to-solve through traditional optimization algorithms therefore proposed algorithm is utilized. Maximizing the heat transfer coefficient is formulated by the following equation:

$$F_1 = \arg \max U(X), X = [x_1, x_2, \dots, x_D], \quad x_{i,\min} \leq x_i \leq x_{i,\max}, i = 1, 2, \dots, D \tag{78}$$

With subject to given set of constraints (n):

$$g_j(X) \leq 0, j = 1, 2, 3, \dots, n \tag{79}$$

Second of objective of this problem is to minimize the total cost of the spiral heat exchanger as formulated below:

$$F_2 = \arg \min C_{tot}(Y), \quad Y = [y_1, y_2, \dots, y_D] \\ y_{i,\min} \leq y_i \leq y_{i,\max}, i = 1, 2, \dots, D \tag{80}$$

With subject to given set of constraints (n):

$$g_j(Y) \leq 0, \quad j = 1, 2, 3, \dots, n \tag{81}$$

Original multi objective optimization problem is converted to single objective problem via weighted sum method. Normalized multi objective optimization is put into practice with taking into account of varying weighted factors to both objectives and formulation of the single objective problem becomes:

$$\arg \min f(F_1, F_2) = w_1(F_2/F_{2,\min}) - (1 - w_1)(F_1/F_{1,\max}) \\ + \sum_{i=1}^n R_1(g_i(X)) + \sum_{i=1}^n R_2(g_i(Y)) \tag{82}$$

**Table 3** Upper and lower bounds of design variables [44]

	Lower bound	Upper bound
$\Delta P_h$ —pressure drop in hot side (kPa)	0.0	172.5
$\Delta P_c$ —pressure drop in cold side (kPa)	0.0	172.5
$D_s$ —outer spiral diameter (m)	0.5	1.5
L—length (m)	5.0	22.0
H—width (m)	0.05	2.3
$b_h$ —hot side plate spacing (m)	0.005	0.032
$b_c$ —cold side plate spacing (m)	0.005	0.032

where  $w_1$  is a weighted factor for the first objective function and can be decided by the designer’s choice. Assigning proper values (between 0.0 and 1.0) to  $w_1$  results in construction of Pareto front which is a set of optimum solutions.  $F_{1,\max}$  and  $F_{2,\min}$  are the extremum values of the objective functions of  $F_1$  and  $F_2$ , correspondingly. In order to account for the problem constraints during the optimization process, static penalty method is applied. Static penalty method is a favorable choice in handling of constraint violation due to its simplicity and easy implementation for any kind of optimization problem. R1 is the static penalty coefficient with having relatively large value. Low value of R1 leads to exploring unfeasible regions of the search space and constraint violation can be easily observed. Giving high value to R1 causes more function evaluations to obtain optimum value which requires relatively high computational cost. Therefore, problem-dependent coefficients should be tried and trial-and-error method should be applied to acquire the proper R1 value on the course of iterations.

Heat exchanger design is a tedious and challenging task. A designer decides the application area of the intended heat exchanger. In some industries such as food processing, maximum heat transfer rate is more important than the total cost [44]. In some cases, designer should consider the total cost rather than heat transfer rates according to the customer’s needs. However, both heat transfer and total cost are essential considerations in design procedure. In this study, GBA will be utilized to obtain the objectives including the minimum total cost of heat exchangers and the maximum total heat transfer coefficient separately. Finally, Pareto frontier formed by the non-dominated solutions of conflicting objectives will be constructed and best solution will be decided through the most prevalent decision making methods including LINMAP, TOPSIS, and Shannon entropy approach. Interested readers can refer to Ahmadi et al. [59] for further information in decision-making approaches.

Table 2 reports the average thermophysical properties of the fluids used in this case study. Table 3 shows the upper and lower bounds of the search space. Overall heat transfer coefficient optimization results obtained from GBA, ACS,

**Table 4** Comparison of the algorithms for maximizing overall heat transfer coefficient

	Case study [46]	GBA	ACS	ITHS	QPSO
$\Delta P_c$ (kPa)	85.43	172.2314	163.0104	95.8807	52.6694
$\Delta P_h$ (kPa)	110.19	171.4592	172.1316	167.1749	166.9380
$D_s$ (m)	0.849	0.7579	0.7032	0.6953	0.5408
H (m)	0.9144	0.7029	0.7685	0.8028	1.1405
L (m)	7.817	8.5641	7.9086	7.7782	5.6279
$b_h$ (m)	0.0318	0.0319	0.0282	0.0272	0.0163
$b_c$ (m)	0.0063	0.0055	0.0050	0.0061	0.0050
$C_i$ (€)	28,211.86	25,494.9092	25,638.3990	26,051.8224	26,477.7611
$C_o$ (€/year)	15,414.17	25,241.8715	24,794.9273	22,568.6924	21,493.3930
$C_{od}$ (€)	117,241.46	191,991.6815	188,592.1898	171,659.2687	163,480.4564
$C_{tot}$ (€)	145,453.32	217,486.5908	214,230.5888	197,711.0912	189,958.2176
U (W/m <sup>2</sup> K)	1118.62	1300.189	1287.8813	1253.1643	1219.4561

ITHS, QPSO algorithms along with the results in [46] are given in Table 4. As shown in Table 4, GBA outperforms other algorithms in terms of best results. As compared to case study, increment in pressure drop in hot side (55.9 %) and cold side (101.6 %) is caused by the considerable increase of the mean velocity of the working fluids in both sides. This velocity increase leads to a marked rise in heat transfer coefficients of both and cold sides which enhances heat transfer mechanism by increasing overall heat transfer coefficient values. On the contrary, increase in heat transfer rates brings about a significant rise (49.5 %) in total cost of heat exchanger due to the effect of remarkable increase in pressure drop rates. Figure 3 shows the convergence histories of the design variables for this case. Figure 4 also depicts the instance of the evolution of the objective function for maximizing overall heat transfer coefficient.

As total cost is comprised of capital and operational costs, algorithm evaluates both these costs simultaneously when cost is chosen as an objective function. As formulated in Eq. (61), total capital cost is a function of heat exchanger area and therefore algorithm tends to optimize this value by selecting proper values from the search space. Operational cost rates are heavily dependent of pressure losses for both hot and cold streams. Therefore, proper tuning should be made by the algorithm for design those variables having direct relations with pressure drop. Algorithm optimizes the total cost through increasing width and plate spacing so as to enhance free flow area which causes, at constant mass flow rates, considerable decrease in mean flow velocities. Table 5 gives the best results related to minimizing total cost of spiral heat exchanger. Substantial decrease in pressure drop in hot (91.1 %) and cold (90.8 %) sides brings about an enormous decline (91.3 %) in total discounted operating cost values. Increase in total heat transfer surface area (66.3 %) induces a moderate rise in investment cost rates. All in all, total cost of heat exchanger shows a considerable decline (66.5 %),

and reduces to 48,563.76 € when GBA is applied. Figure 5 shows the convergence characteristics of the design variables for this case. Figure 6 visualizes the convergence history of the objective function for minimum cost.

Single objective optimization results for minimum total cost and maximum overall heat transfer coefficients show that higher total costs result in lower heat transfer rates or vice versa. Therefore, there occurs a strong necessity to implement multi objective optimization. For this aim, multi objective global best algorithm (MO-GBA) is utilized to obtain simultaneous optimum results of objective functions. Figure 7 shows the Pareto optimum curve and some of the Pareto-optimal points obtained by using proposed MO-GBA. At design point A, overall heat transfer coefficient is at its minimum while total cost of heat exchanger is 48,563.7627 € which is of its best value among the set of optimum solutions. At design point F, Overall heat transfer coefficient is at its highest value corresponding to 1300.189 W/m<sup>2</sup>K while total cost is 217,486.5908 €. Table 6 reports some of the sample points of the Pareto frontiers shown in Fig. 7. As stated in Table 6, pressure drop values for both hot and cold sides increase when we move from the design point A to F on the Pareto front. It is this cumulative increase which leads to give a marked rise in total cost and heat transfer rates. Figure 7 also shows the optimal solutions selected by the LINMAP, TOPSIS, and Shannon's entropy decision making methods. Ideal and non-ideal solution points for two objectives of spiral heat exchanger design are also specified in Fig. 7. Optimal points along with their corresponding deviation indexes obtained through aforementioned decision making methods are given in Table 7. Deviation index is an important factor that determines the suitability of a particular decision making method for a particular optimization problem. Some of the decision making methods calculates Euclidian distance of each optimal solution on the Pareto frontier

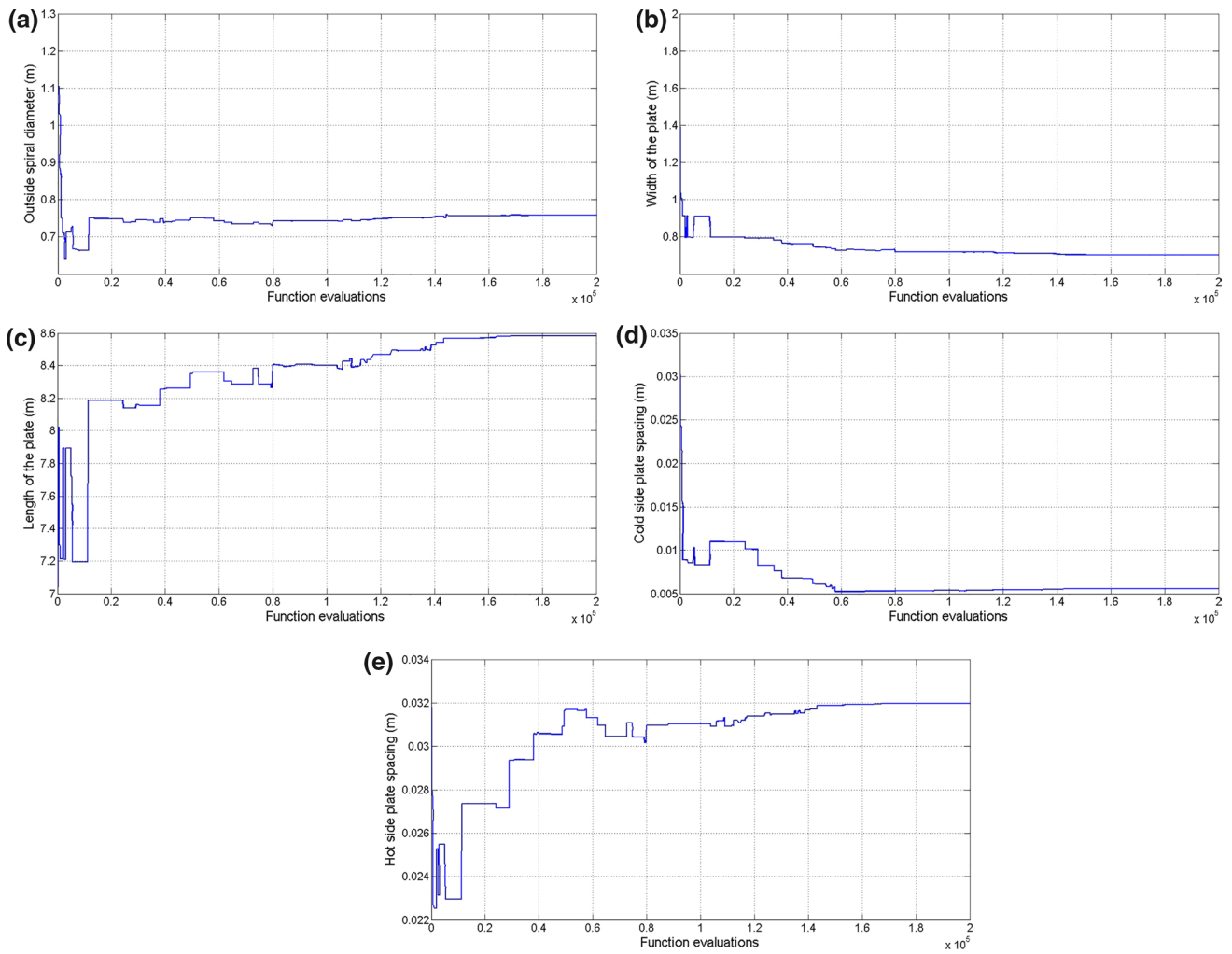
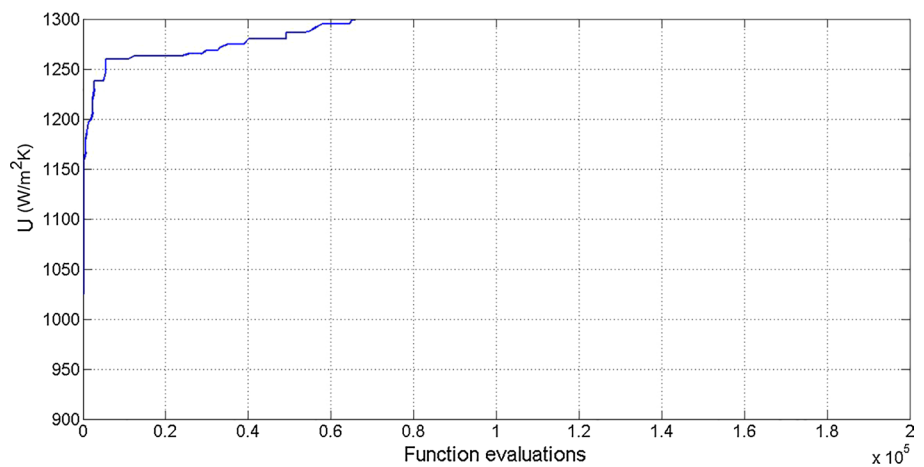


**Fig. 3** Evolution histories of the decision variables of spiral heat exchangers for maximization of overall heat transfer coefficient

**Fig. 4** Convergence history of the objective function for maximization of overall heat transfer coefficient



from the ideal or nadir points. For instance, LINMAP uses ideal solution in deciding optimum solution while TOPSIS using non-ideal (nadir) solution. Comparison among the

different results obtained from these three different decision making methods is maintained by the deviation index, which is calculated as [60]

**Table 5** Comparison of the algorithms for minimizing total cost of heat exchanger

	Case study [46]	GBA	ACS	ITHS	QPSO
$\Delta P_c$ (kPa)	85.43	7.8479	7.4341	4.1222	5.8250
$\Delta P_h$ (kPa)	110.19	9.8028	9.8318	10.6633	9.9424
$D_s$ (m)	0.849	0.6226	0.6241	0.6439	0.6315
$H$ (m)	0.9144	2.3000	2.2996	2.2670	2.2999
$L$ (m)	7.817	5.1688	5.1820	5.3597	5.2424
$b_h$ (m)	0.0318	0.0319	0.0319	0.0317	0.0320
$b_c$ (m)	0.0063	0.0061	0.0063	0.0087	0.0071
$U$ (W/m <sup>2</sup> K)	1118.62	658.4915	656.9083	644.2217	649.2418
$C_i$ (€)	28,211.86	38,087.9621	38,142.0923	38,582.4503	38,407.2075
$C_o$ (€/year)	15,414.17	1377.2930	1370.7909	1387.6348	1345.2113
$C_{od}$ (€)	117,241.46	10,475.8006	10,426.3449	10,554.4608	10,231.7842
$C_{tot}$ (€)	145,453.32	48,563.7627	48,568.4372	49,136.9111	48,638.9918

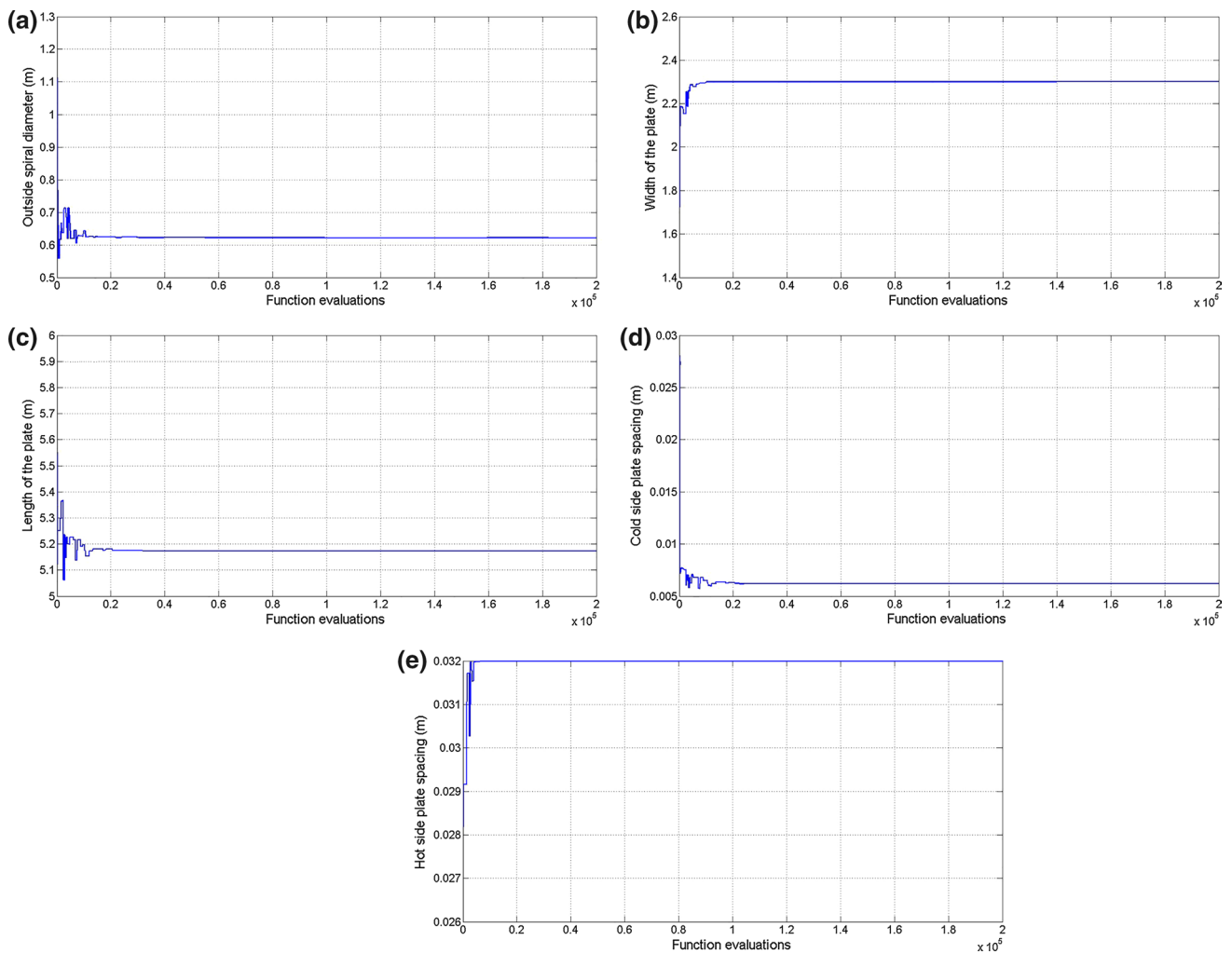


**Fig. 5** Evolution histories of the decision variables of spiral heat exchangers for minimization of total cost

**Fig. 6** Convergence history of the objective function for minimization of total cost of heat exchanger

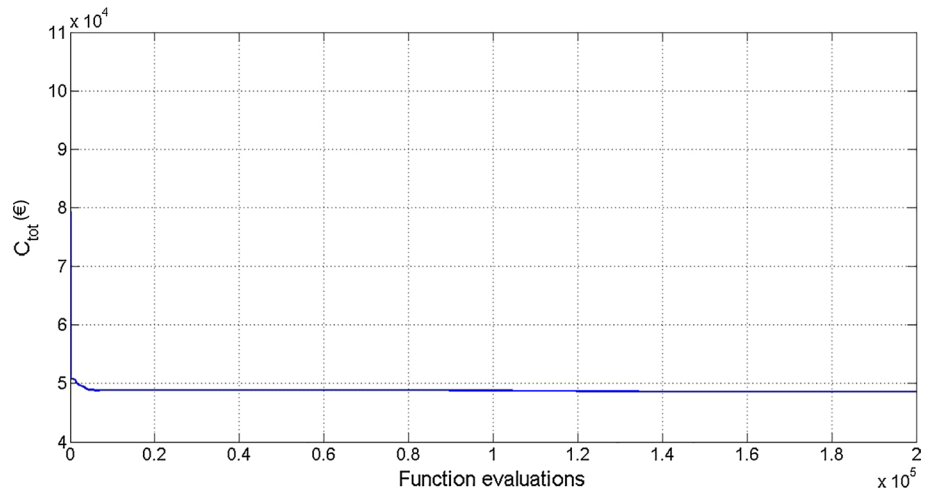


**Fig. 7** Pareto optimum curve and some of the Pareto-optimal points obtained by using MO-GBA

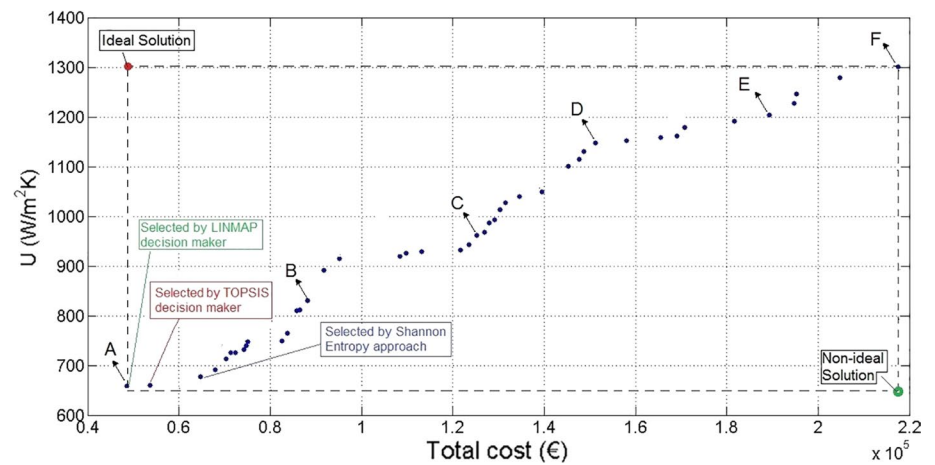


**Table 6** Optimum design variables of the some of the Pareto-optimal points shown in Fig. 7

	A	B	C	D	E	F
$\Delta P_c$ (kPa)	7.8479	1.3281	2.7575	36.1361	38.1671	172.13
$\Delta P_h$ (kPa)	9.8028	59.4918	102.384	127.225	168.879	172.41
$D_s$ (m)	0.6226	0.8413	0.8885	0.7262	0.7512	0.7579
$H$ (m)	2.3000	1.2894	0.9878	0.8815	0.7919	0.7029
$L$ (m)	5.1688	7.3132	8.2406	7.7326	8.2143	8.5641
$b_h$ (m)	0.0319	0.0275	0.0291	0.0283	0.0282	0.0319
$b_c$ (m)	0.0061	0.0317	0.0305	0.0091	0.0102	0.0055
$C_i$ (€)	38,087.96	33,222.20	30,462.37	27,432.80	26,686.64	25,494.90
$C_o$ (€/year)	1377.293	7237.1633	12,466.45	16,283.39	21,377.22	25,241.87
$C_{od}$ (€)	10,475.80	55,046.44	94,820.85	123,852.79	162,596.84	191,991.68
$C_{tot}$ (€)	48,563.76	88,268.65	125,283.22	151,285.59	189,283.48	217,486.59
$U$ (W/m <sup>2</sup> K)	658.49	830.14	961.58	1148.38	1203.314	1300.18

$$d = \frac{\sqrt{\sum_{j=1}^n (F_{ij} - F_j^{ideal})^2}}{\sqrt{\sum_{j=1}^n (F_{ij} - F_j^{ideal})^2 + \sum_{j=1}^n (F_{ij} - F_j^{nadir})^2}} \quad (83)$$

where  $n$  denotes the number of objectives and  $i$  represents each solution on the Pareto frontier.  $F$  is Euclidian non-dimensional objective function;  $F^{ideal}$  and  $F^{nadir}$  are the corresponding values of objective functions at the ideal and nadir points, respectively. If the value of deviation

index is low, then it is close to the ideal point and far from the nadir point. Based on these explanations, we can conclude that optimum solution decided by LINMAP is more relevant since its deviation index is the lowest

among the results obtained from the other decision making methods.

### 4.2 Results of the heat pipe optimization

**Table 7** Comparison between optimal solutions obtained from TOPSIS, LINMAP and Shannon’s entropy methods

	LINMAP	TOPSIS	Shannon’s entropy
$\Delta P_c$ (kPa)	7.8479	1.7390	0.5975
$\Delta P_h$ (kPa)	9.8028	16.6323	29.498
$D_s$ (m)	0.6226	0.6794	0.7408
H (m)	2.3000	2.0716	1.9184
L (m)	5.1688	5.7211	6.0228
$b_h$ (m)	0.0319	0.0286	0.0238
$b_c$ (m)	0.0061	0.0152	0.0288
$C_i$ (€)	38,087.96	38,020.159	37,453.92
$C_o$ (€)	1377.293	2056.449	3587.003
$C_{od}$ (€)	10475.80	15,641.515	27,283.030
$C_{tot}$ (€)	48,563.76	53,661.675	64,736.957
U (W/m <sup>2</sup> K)	658.49	660.483	677.494
Deviation index	0.2939	0.3292	0.4274

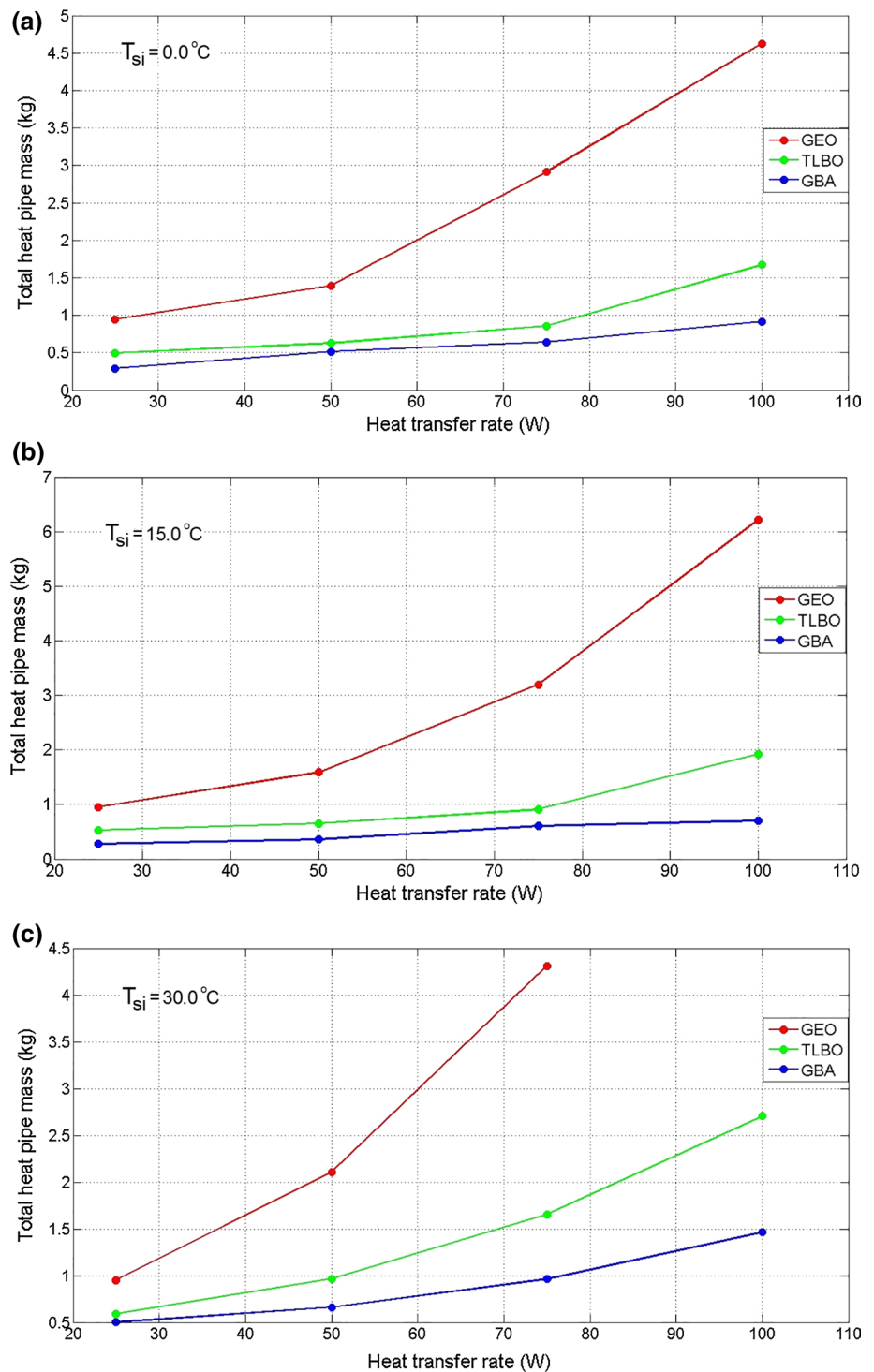
Table 8 reports the optimal results attained by the proposed GBA from fifty independent algorithm runs and results obtained by Rao and More [31] via Teaching Learning Based Optimization (TLBO). As it is observed from Table 8, GBA finds better results than TLBO algorithm in terms of minimum heat pipe mass values. It is expected to see that total mass of heat pipe increases as total heat load Q increases. Moreover, increase in the temperature on the outside surface of condenser section  $T_{si}$  causes heavier HP. It is interesting to observe that the values of D and  $d_v$  are very close to the lower bound of allowable constraints. In order to obtain minimum total weight, algorithm tends to obtain higher porosity rates which is caused by lower values of N and D. However, higher porosity values is not feasible in technological terms [47]. Figure 8a–c compares the optimum results found by TLBO [31], Generalized Extremal Optimization (GEO) [31], and GBA for different heat loads for different working temperatures. As it is observed, GBA

**Table 8** Comparison of optimal results obtained from GBA and TLBO

Q (W)	°C	Method	N	D (m)	$d_v$ (m)	$t_w$ (m)	$L_e$ (m)	$L_c$ (m)	$t_l$ (m)	$\epsilon$	$m_{total}$ (kg)
25	0	TLBO	4271	3.007e−5	0.0287	7.356e−5	0.0668	0.0512	1.094e−3	0.9162	0.5084
		GBA	3700	2.591e−4	0.0388	9.927e−4	0.0630	0.0642	3.221e−4	0.9661	<b>0.2904</b>
50	0	TLBO	1681	3.639e−5	0.0329	9.094e−5	0.1742	0.0542	1.018e−3	0.9469	0.6359
		GBA	1796	3.547e−4	0.0403	8.811e−4	0.1683	0.1044	3.001e−4	0.6913	<b>0.5146</b>
75	0	TLBO	6390	3.673e−5	0.0392	8.866e−5	0.1081	0.1151	1.158e−3	0.9315	0.8532
		GBA	7176	6.602e−5	0.0588	0.0012	0.1524	0.2292	3.002e−4	0.9524	<b>0.6406</b>
100	0	TLBO	7551	2.582e−5	0.0386	9.702e−5	0.0686	0.0562	2.571e−3	0.9567	1.6575
		GBA	3576	1.802e−4	0.0640	7.540e−4	0.3663	0.1011	3.066e−4	0.7156	<b>0.9148</b>
25	15	TLBO	8612	2.9664e−5	0.0297	6.9900e−5	0.0793	0.0931	1.028e−3	0.9811	0.5234
		GBA	10,641	4.741e−5	0.04218	1.514e−4	0.1422	0.1632	3.019e−4	0.9664	<b>0.2785</b>
50	15	TLBO	1401	3.4418e−5	0.0393	9.7385e−5	0.0785	0.0585	1.0099e−3	0.8845	0.6593
		GBA	14,680	6.263e−5	0.04407	5.185e−5	0.3169	0.2015	3.035e−4	0.9063	<b>0.3566</b>
75	15	TLBO	1494	2.9830e−5	0.0398	8.9351e−5	0.1334	0.1624	1.1141e−3	0.9604	0.9140
		GBA	3158	5.370e−5	0.06357	5.100e−4	0.2814	0.2259	3.013e−4	0.9654	<b>0.6037</b>
100	15	TLBO	6819	2.7130e−5	0.0333	7.3836e−5	0.1347	0.1209	2.8191e−3	0.9197	1.9254
		GBA	7333	9.398e−5	0.05329	9.543e−4	0.3316	0.1316	3.009e−4	0.8476	<b>0.7017</b>
25	30	TLBO	5384	3.4309e−5	0.0326	7.4947e−5	0.0943	0.0713	1.0217e−3	0.9202	0.5771
		GBA	4754	1.924e−4	0.03636	0.0013	0.1207	0.2178	3.016e−4	0.8534	<b>0.5015</b>
50	30	TLBO	4565	4.3306e−5	0.0334	9.8401e−5	0.1660	0.0800	1.4708e−3	0.9934	0.9617
		GBA	11,880	6.908e−5	0.05331	0.0011	0.2435	0.2752	3.003e−4	0.9538	<b>0.6639</b>
75	30	TLBO	7450	2.6820e−5	0.0405	9.4628e−5	0.0676	0.0496	2.4710e−3	0.9467	1.6426
		GBA	6474	1.223e−4	0.05371	0.0012	0.3422	0.2954	3.005e−4	0.8280	<b>0.9626</b>
100	30	TLBO	4579	2.6571e−5	0.0382	9.0315e−5	0.1602	0.1987	3.0047e−3	0.5889	2.6856
		GBA	7631	9.727e−5	0.07796	0.0013	0.1843	0.3312	3.011e−4	0.7727	<b>1.4598</b>

Bold values represent better output between two compared result for the related case study

**Fig. 8** Minimum mass of heat pipes for varying heat loads for different condenser wall temperatures



finds better results than literature studies with respect to minimum heat pipe weights for each case study. Figure 9a–c show convergence characteristics of the GBA algorithm for different temperatures of outside surface of the condenser section. For each case in Fig. 9, a sharp decline in objective function value is seen at the early stages and it continues with gradual decreases till the end of the iterations.

## 5 Conclusion

In this study, investigation on the efficient design of spiral heat exchangers and heat pipes is developed by the stochastic-based optimization method of global best algorithm. GBA is a derivative free stochastic optimization method which is guided by the global best solution obtained during

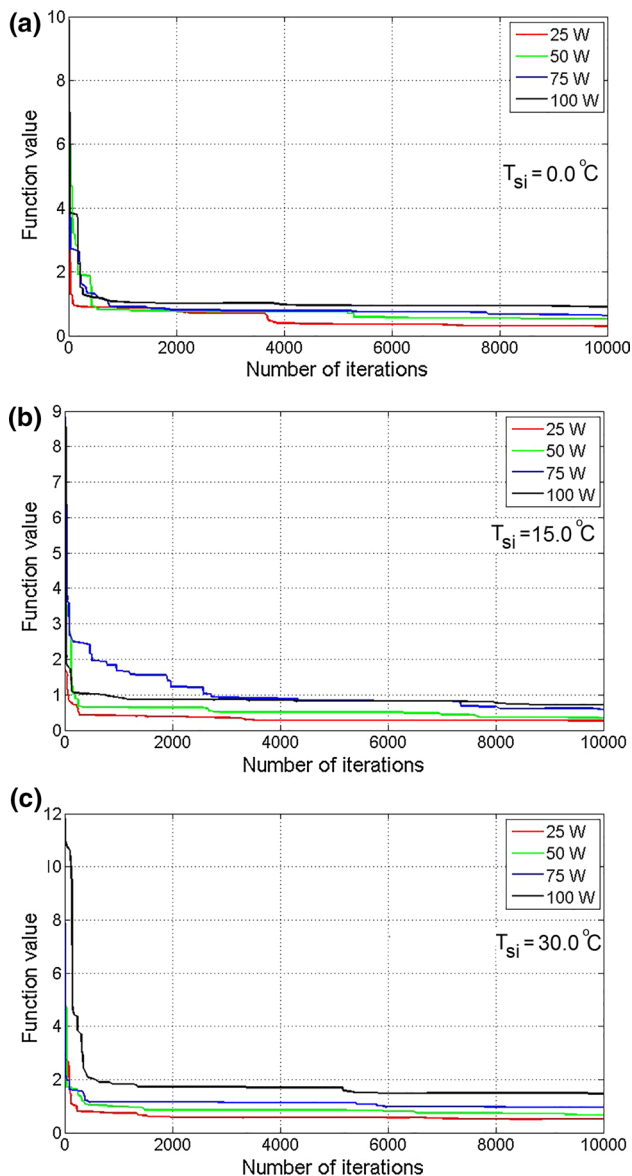


**Fig. 9** Convergence characteristics of the minimum HP mass acquired by GBA for different heat transfer rates and operating conditions

iterations. Both design problems are highly nonlinear and involve binding problem constraints, which makes them hard-to-solve for any kind of optimizer available in the literature. Effectivity of the proposed GBA is assessed by means of the optimal results obtained from multi objective optimization analysis of spiral heat exchangers and single objective optimization of heat pipes. GBA shows superior performance for both optimization cases as it not only outperforms the literature studies with respect to optimum results it attains. But also proves its applicability on thermal-energy systems. For a future work, utilization of GBA

can be extended to multi objective optimization of thermo-dynamic cycles which has become a hot spot research topic in thermal systems.

## References

- Sanaye S, Modarrespoor D (2014) Thermal-economic multi objective optimization of heat pipe heat exchanger for energy recovery in hvac application using genetic algorithm. *Therm Sci* 18:375–391
- Ozkol I, Komurgoz G (2005) Determination of the optimum geometry of the heat exchanger body via genetic algorithm. *Int J Heat Mass Transf* 48:283–296
- Hilbert R, Janiga G, Baron R, Thevenin D (2006) Multiobjective shape optimization of a heat exchanger using parallel genetic algorithm. *Int J Heat Mass Transf* 49:2567–2577
- Xie GN, Sunden B, Wang QW (2008) Optimization in calculation of shell and tube heat exchanger by a genetic algorithm. *Appl Therm Eng* 28:895–906
- Sun S, Lu Y, Yan C (1993) Optimization in calculation of shell and tube heat exchanger. *Int Commun Heat Mass* 20:675–685
- Ponce-Ortega JM, Serna-Gonzalez M, Jimenez-Gutierrez A (2009) Use of genetic algorithms for the optimal design of shell and tube heat exchangers. *Appl Therm Eng* 29:203–209
- Wildi-Tremblay P, Gosseling L (2007) Minimizing shell and tube heat exchanger cost with genetic algorithms and considering maintenance. *Int J Energy Res* 31:867–885
- He D, Wang F, Mao Z (2008) A hybrid genetic algorithm approach based on differential evolution for economic dispatch with valve-point effect. *Int J Electr Power* 30:31–38
- Babu BV, Munawar SA (2007) Differential evolution strategies for optimal design of shell-and-tube heat exchanger. *Chem Eng Sci* 62:3720–3739
- Thuy NTP, Pendyala R, Marneni N (2014) Heat exchanger network optimization using differential evolution with stream splitting. *Appl Mech Mater* 625:373–377
- Ayala HVM, Keller P, Morais MF, Mariani VC, Coelho LS, Rao RV (2016) Design of heat exchangers using a novel multi objective free search differential evolution paradigm. *Appl Therm Eng* 94:170–177
- Rao RV, Patel VK (2011) Optimization of mechanical draft counter flow wet-cooling tower using artificial bee colony algorithm. *Energy Conversat Manag* 52:2611–2622
- Şahin AŞ, Kılıç B, Kılıç U (2011) Design and economic optimization of shell and tube heat exchangers using artificial bee colony (ABC) algorithm. *Energy Conversat Manag* 52:3356–3362
- Labbi Y, Attous DB, Mahdad B (2014) Artificial bee colony optimization for economic dispatch with valve point effect. *Front Energy* 8:449–458
- Kim K, Lee KH, Baek SW (2013) A study on heat pipe optimization using PSO. *IJCEE* 5:291–293
- Rao RV, Patel V (2010) Thermodynamic optimization of cross flow plate-fin heat exchanger using a particle swarm optimization algorithm. *Int J Therm Sci* 49:1712–1721
- Patel VK, Rao RV (2010) Design optimization of shell-and-tube heat exchanger using particle swarm optimization technique. *Appl Therm Eng* 30:1417–1425
- Jalilrad S, Cheraghali MH, Ashtiani HAD (2015) Optimal design of shell-and-tube heat exchanger based on particle swarm optimization technique. *J Comput Appl Mech* 46:21–29
- Blum C, Roli A (2003) Metaheuristic in combinatorial optimization: overview and conceptual comparison. *ACM Comput Surv* 35:268–308

20. Egner MW, Burmeister LC (2005) Heat transfer for laminar flow spiral ducts of rectangular cross section. *J Heat Transf* 127:352–356
21. Trom L (1995) Use spiral plate exchangers for various applications. *Hydrocarb Process* 74:73–81
22. Wilhelmsson B (2005) Consider spiral heat exchangers for fouling application. *Hydrocarb Process* 84:81–83
23. Picon-Núñez M, Canizalez-Davalos L, Martínez-Rodríguez G, Polley GT (2007) Shortcut design approach for spiral heat exchangers. *Food Bioprod Process* 85:322–327
24. Picon-Núñez M, Canizalez-Davalos L, Medina-Flores JM (2009) Alternative sizing methodology for compact heat exchangers of the spiral type. *Heat Transf Eng* 30:744–750
25. Naphon P, Wongwises S (2002) An experimental study on the in-tube convective heat transfer coefficient in a spiral coil heat exchanger. *Int Commun Heat Mass Transf* 29:797–809
26. Bes Th, Roetzel W (1992) Distribution of heat flux density in spiral heat exchangers. *Int J Heat Mass Transf* 35:1331–1347
27. Li H, Nagano K, Lai Y (2012) A new model and solutions for a spiral heat exchanger and its experimental validation. *Int J Heat Mass Transf* 55:4404–4414
28. Burmeister LC (2006) Effectiveness of a spiral-plate heat exchanger with equal capacitance rates. *J Heat Transf* 128:295–301
29. Lu X, Du X, Zeng M, Zhang S, Wang Q (2014) Shell-side thermal-hydraulic performances of multilayer spiral-wound heat exchangers under different wall thermal boundary conditions. *Appl Therm Eng* 70:1216–1227
30. de Sousa FL, Vlassov V, Ramos FM (2004) Generalized extremal optimization: an application in heat pipe design. *Appl Math Model* 28:911–931
31. Rao RV, More KC (2015) Optimal design of heat pipe using TLBO (teaching-learning-based- optimization) algorithm. *Energy* 80:535–544
32. Said SA, Akash BA (1999) Experimental performance of a heat pipe. *Int Commun Heat Mass Transf* 26:679–684
33. Kim SJ, Seo JK, Do KH (2003) Analytical and experimental investigation on the operational characteristics and thermal optimization of a miniature heat pipe with a grooved structure. *Int J Heat Mass Transf* 46:2051–2063
34. Shi PZ, Chua KM, Wong YM, Tan YM (2006) Design and performance optimization of miniature heat pipes in LTCC. *J Phys: Conf Ser* 34:142–147
35. Vlassov VV, Souza FL, Takahashi WK (2006) Comprehensive optimization of a heat pipe radiator assembly filled with ammonia or acetone. *Int J Heat Mass Transf* 49:4584–4595
36. Maheshkumar P, Muraleedharan C (2011) Minimization of entropy generation in flat heat pipe. *Int J Heat Mass Transf* 54:645–648
37. Agha SR (2011) Heat pipe performance optimization: a taguchi approach. *J Res Mech Eng Technol* 31:3410–3419
38. Lips S, Lefevre F (2011) A general analytical model for the design conventional heat pipes. *Int J Heat Mass Transf* 72:288–298
39. Cui X, Zhu Y, Li Z, Shun S (2014) Combination study of operation characteristics and heat transfer mechanism for pulsating heat pipe. *App Therm Eng* 65:394–402
40. Nithyanandam K, Pitchumani R (2011) Analysis and optimization of a latent thermal energy storage system with embedded heat pipes. *Int J Heat Mass Transf* 54:4596–4610
41. Morawietz K, Hermann M (2014) Integrated development and modelling of heat pipe solar collectors. *Energy Procedia* 48:157–162
42. Roper CS (2011) Multi-objective optimization for design of multifunctional sandwich panel heat pipes with micro-architected truss cores. *Int J Heat Fluid Flow* 32:239–248
43. Zhang C, Chen Y, Shi M, Peterson GP (2009) Optimization of heat pipe with axial “Ω” shaped micro grooves based on a niched Pareto genetic algorithm (NPGA). *Appl Therm Eng* 29:3340–3345
44. Bidabadi M, Sadaghiani AK, Vahdat Azad A (2013) Spiral heat exchanger optimization using genetic algorithm. *Sci Iran* 20:1445–1454
45. Storn R, Price K (1997) Differential evolution - a simple and efficient heuristic for global optimization over continuous spaces. *J Glob Optim* 11:341–359
46. Moretta AA (2010) Spiral plate heat exchangers: sizing units for cooling non-Newton slurries. *Chem Eng* 5:44–49
47. de Souza FL, Vlassov VV (2004) Heat pipe design through generalized extremal optimization. *Heat Transf Eng* 25:34–45
48. Morimoto E, Hotta K (1988) Study of the geometric structure and heat transfer characteristics of a spiral plate heat exchanger. *Heat Transf Jpn Res* 17:53–71
49. Perry RH, Green DW (1997) Perry’s chemical engineers’ handbook. McGraw-Hill, New-York
50. Minton PE (1970) Designing spiral heat exchangers. *Chem Eng* 4:103–112
51. Hall SG (1990) Capital cost targets for heat exchanger networks comprising mixed materials of construction, pressure ratings and exchangers types. *Comput Chem Eng* 14:319–325
52. May R (1976) Simple mathematical models with very complicated dynamics. *Nature* 261:459–467
53. Brest J, Greiner G, Boscovic B, Mernik M, Zumer V (2006) Self-adaptive control parameters in differential evolution: a comparative study on numerical benchmark problems. *IEEE Trans Evol Comput* 10:646–657
54. Opitz D, Maclin R (1999) Popular ensemble methods: an empirical study. *J Artif Intell Res* 11:169–198
55. Civicioglu P (2013) Artificial cooperative search algorithm for numerical optimization problems. *Inf Sci* 229:58–76
56. Yadav P, Kumar R, Panda SK, Chang CS (2012) An intelligent tuned harmony search algorithm for optimization. *Inf Sci* 196:47–72
57. Sun J, Feng B, Xu W (2004) Particle swarm optimization with particles having quantum behaviour. In: Proceedings of congress on evolutionary computation, Portland, OR, USA, pp 325–331
58. Sun J, Xu W, Feng B (2005) Adaptive parameter control for quantum behaved particle swarm optimization on individual level. In: Proceedings of IEEE international conference on systems, man and cybernetics, Big Island, HI, USA, pp 3049–3054
59. Ahmadi MH, Sayyaadi H, Dehghani S, Hosseinzade H (2013) Designing a solar powered Stirling heat engine based on multiple criteria: maximized thermal efficiency and power. *Energy Convers Manag* 75:282–291
60. Kumar R, Kaushik SC, Kumar R, Hans R (2016) Multi-objective thermodynamic optimization of an irreversible regenerative Brayton cycle using evolutionary algorithm and decision making. *Ain Shams Eng J* 7:741–753